Published in final edited form as:
Dev Biol. 2010 August 15; 344(2): 669–681. doi:10.1016/j.ydbio.2010.05.496.

Mesodermal *Tbx1* is required for patterning the proximal mandible in mice

Vimla S. Aggarwal[1,*], **Courtney Carpenter**[2], **Laina Freyer**[1], **Jun Liao**[1,#], **Marilena Petti**[1], and **Bernice E. Morrow**[1,†]

[1]Department of Molecular Genetics, Albert Einstein College of Medicine, 1300 Morris Park Avenue, Bronx, NY 10461, USA.

[2]Department of Surgery, Montefiore Medical Center, 111 East 210th Street, Bronx, NY 10467, USA.

Abstract

Defects in the lower jaw, or mandible, occur commonly either as isolated malformations or in association with genetic syndromes. Understanding its formation and genetic pathways required for shaping its structure in mammalian model organisms will shed light into the pathogenesis of malformations in humans. The lower jaw is derived from the mandibular process of the first pharyngeal arch (MdPA1) during embryogenesis. Integral to the development of the mandible, is the signaling interplay between *Fgf8* and *Bmp4* in the rostral ectoderm and their downstream effector genes in the underlying neural crest derived mesenchyme. The non-neural crest MdPA1 core mesoderm is needed to form muscles of mastication, but its role in patterning the mandible is unknown. Here, we show that mesoderm specific deletion of *Tbx1*, a T- box transcription factor and gene for velo-cardio-facial/DiGeorge syndrome, results in defects in formation of the proximal mandible by shifting expression of *Fgf8*, *Bmp4* and their downstream effector genes in mouse embryos at E10.5. This occurs without significant changes in cell proliferation or apoptosis at the same stage. Our results elucidate a new function for the non-neural crest core mesoderm and specifically, mesodermal *Tbx1*, in shaping the lower jaw.

Keywords

Mandible; velo-cardio-facial syndrome; mouse model; pharyngeal apparatus; mandibular arch; organogenesis; Tbx1

INTRODUCTION

The mandible, or lower jaw forms via complex tissue interactions within the pharyngeal apparatus. During early mammalian embryonic development, the mandibular component of the first pharyngeal arch (MdPA1) can be observed on either side of the head as bilaterally

†Author for correspondence: bernice.morrow@einstein.yu.edu.
*Present Address: Department of Pathology, Columbia University Medical Center, 630 W. 168th Street, New York, NY 10032, USA.
#Present address: Department of Molecular, Cellular and Developmental Biology, Yale University, P. O. Box 208103, New Haven, CT 06520, USA.

symmetrical bulges within the pharyngeal apparatus. Each pharyngeal arch is composed of tissues of various embryonic origins. The ectoderm of each arch lines the outer surface, while the endoderm is continuous with the foregut internally. The mesenchyme of the mandibular processes is derived from the cranial neural crest cells and paraxial core mesoderm (Graham, 2003). The cranial neural crest is a migratory cell population that detaches from the dorsal neural tube and migrates into the pharyngeal apparatus to sequentially form distinct arches (Santagati and Rijli, 2003). Proper spatial and temporal patterning of the MdPA1 is crucial for morphogenesis of derivatives like the skeletal elements of the mandible (which include the dentary, tympanic ring and the malleus) and teeth. Chondrogenesis of the neural crest mesenchyme involves the formation of Meckel's cartilage (Hall, 1980) as well as the secondary cartilage forming the coronoid, condylar and angular cartilages (proximal mandible; Beresford, 1975). Later the lower jaw forms from ossification of cartilaginous tissues.

Many genetic syndromes affecting newborns have associated craniofacial malformations. One such syndrome is termed velo-cardio-facial syndrome/DiGeorge syndrome (VCFS/DGS; MIM # 92430/188400) associated with 1.5-3 million base pair hemizygous 22q11.2 deletions. Affected individuals have a characteristic facial appearance consisting of a long face, flattening of the cheeks caused in part by muscle hypotonia, allergic shiners under the eyes and small appearing lower jaw (retrognathia) caused by platybasia (Butts, 2009). In addition, they have a prominent nose with narrow nasal passages, small, posteriorly rotated ears as well as a submucous or occult submucous cleft palate. The craniofacial anomalies are frequently accompanied by hypernasal speech and velo-pharyngeal insufficiency (Havkin et al., 2000). As the malformations in association with the syndrome occur commonly as isolated defects, understanding the molecular pathogenesis of the syndrome would provide insights into the isolated developmental defects. Within the 22q11.2 region hemizygously deleted in patients is the *TBX1* gene, encoding a member of the T-box family of dosage sensitive transcription factors. Haploinsufficiency of *TBX1* is believed to be responsible for most of the physical defects in patients including craniofacial anomalies (Jerome and Papaioannou, 2001; Lindsay et al., 2001; Merscher et al., 2001). *Tbx1*$^{+/-}$ mice have mild defects at reduced penetrance. *Tbx1* homozygous null mutant mice die at birth displaying most of the defects seen in the syndrome, albeit more severe, including cleft palate, missing middle ear bones, mandibular hypoplasia and missing or abnormal bones in the head and neck (Jerome and Papaioannou, 2001; Lindsay et al., 2001; Merscher et al., 2001). *Tbx1* is expressed in multiple tissues that form the embryonic pharyngeal apparatus.

To understand the pathogenesis of jaw anomalies downstream of *Tbx1*, it is necessary to consider tissue specific signaling pathways and functions. The pharyngeal endoderm and ectoderm have major roles in patterning the underlying neural crest derived mesenchyme, needed to form Meckel's cartilage, underlying the lower jaw (Haworth et al., 2004; Liu et al., 2005). We previously showed a role of the pharyngeal endoderm in shaping the craniofacial skeleton (Arnold et al., 2006). The signaling molecules, *Fgf8* and *Bmp4*, in the rostral MdPA1 ectoderm pattern the mandible and teeth (Haworth et al., 2004). The two restrict each other's expression (Liu et al., 2005). In this report, we show that *Fgf8* and *Bmp4*, as well as genes downstream were shifted in expression proximally when *Tbx1* is inactivated. Surprisingly, *Tbx1* is not expressed in the first arch ectoderm (Arnold et al., 2006). Unexpectedly, when *Tbx1* was inactivated in the non-neural crest cell paraxial mesoderm, a similar shift in gene expression was observed coincident with the same lower jaw defects. *Tbx1* has functions in all the tissues where it is expressed. Our data has important implications for signaling from the core mesoderm needed for shaping the proximal mandible downstream of *Tbx1*.

MATERIALS AND METHODS

Mouse mutants

The following mouse mutant alleles used in this study have been described previously: *Tbx1*$^{+/-}$ (Merscher et al., 2001), *Wnt1-Cre* (Danielian et al., 1998), *R26R* (Soriano, 1999), *Tbx1*^{flox} (Arnold et al., 2006) and *T-Cre* (Perantoni et al., 2005). *Tbx1*$^{+/-}$ mice, used to obtain *Tbx1*$^{-/-}$ embryos, are congenic in the FVB background. To generate *T-Cre;Tbx1*$^{flox/-}$ embryos (*TCre-KO*), *T-Cre* transgenic mice were crossed to *Tbx1*$^{+/-}$ mice, on a mixed C57BL6/Swiss Webster background, to obtain *T-Cre;Tbx1*$^{+/-}$ mice. These mice were then crossed to the *Tbx1*$^{flox/flox}$ mice on a mixed genetic background. Wild-type or heterozygous littermates were used as controls in all experiments. All other mouse strains used were maintained in a mixed C57BL/6/ FVB background. PCR strategies for mouse genotyping have been described in the original reports.

Bone and cartilage staining as well as jaw measurements

Skeletal staining of E17.5 embryos was performed as previously described (Jerome and Papaioannou, 2001). Embryos were dissected and the skin removed followed by fixation in 100% EtOH overnight. Bone and cartilage were stained overnight with Alizarin red and Alcian blue, respectively. Loose tissue was removed by digestion in 2% KOH overnight, followed by destaining in 1% KOH/20% glycerol for 4-7 days. Embryos were transferred to 20% glycerol/20% EtOH overnight, followed by storage in 50% glycerol/50% EtOH. The mandible of three *Tbx1*$^{+/+}$ with *Tbx1*$^{+/-}$ versus *Tbx1*$^{-/-}$ embryos at E17.5 was measured from lateral images of the embryos stained with Alizarin red and Alcian blue. We performed a statistical *t* test between three embryos, head length versus jaw size, each from the two groups and calculated the *p* value.

Histology

Mouse embryos were isolated in PBS and fixed in 10% neutral buffered formalin (Sigma) overnight. Following fixation, the embryos were dehydrated through a graded ethanol series, embedded in paraffin and sectioned at 7- 10 μm. All sections were stained with hematoxylin and eosin using standard protocols.

β-galactosidase staining

Whole embryos (E8.5 to 10.5) were stained for β-galactosidase activity according to standard procedures. Embryos were fixed for 30 minutes in 1% formaldehyde, 0.2% glutaraldehyde in PBS. Fixed embryos were washed three times in PBS. Embryos were stained overnight at room temperature using the standard staining solution (5 mM potassium ferricyanide, 5 mM potassium ferrocyanide, 2 mM $MgCl_2$, 1mg/ ml X- gal in PBS), rinsed twice in PBS and post fixed in formalin. After analysis and photography, stained embryos were dehydrated through graded ethanol steps, embedded in paraffin and sectioned at 10 μm. Sections were counterstained with eosin.

RNA *in situ* hybridization

Whole-mount and tissue section RNA *in situ* hybridization with non-radioactive probes was performed as previously described (Alappat et al., 2005; Nowotschin et al., 2006), using probes for *Lhx6*, *Lhx8*, *Spry1*, *Spry2*, *Erm* (all from Dr. John Hebert), *Ptx1* (from Dr. Malcolm Logan), *Gsc* (from Dr. Hubert Schorle), *Fgf8* (from Dr. Gail Martin), *Bmp4* (from Dr. Karine Rizzoti), *Alx4* (from Dr. Frits Meijlink) and *Tbx1* (Nowotschin et al., 2006).

Proliferation and apoptosis analysis

Tbx1$^{+/+}$ and *Tbx1*$^{-/-}$ embryos were isolated in cold PBS followed by fixation in 4% PFA overnight at 4°C, ethanol dehydration and embedded in paraffin wax. Seven μm thick sections were treated with anti-cleaved Caspase 3 (R&D Systems) 1:1000, or anti-phospho-Histone 3 (Upstate) 1:200 in TBS/0.1% Triton X-100/5% goat serum/2%BSA. Sections were incubated for 1 h at room temperature and visualized with a biotinylated goat anti-rabbit IgG conjugate (1:200; DakoCytomation), avidin–biotin complex/HRP formation (DakoCytomation) and DAB/chromogen reaction (DakoCytomation). The slides were then examined under a Zeiss Discovery. V12 microscope using Zeiss Axiovision software. Pictures of the right first arch were taken separately from the left first arch. For each picture, the "Events" feature was used to keep a running count of each stained cell that was manually marked. A total for each section (both left and right arch) was recorded. The number of counted cells per complete first arch was summed for each embryo. This number was then divided by the number of sections for each respective embryo to give the number of cells/section. An average number of cells/section was calculated for *Tbx1*$^{+/+}$ and *Tbx1*$^{-/-}$ embryos in both proliferation and apoptosis experiments. A student's T-test was then run on the numbers with an accepted p-value of 0.05.

RESULTS

Tbx1$^{-/-}$ embryos have a hypoplastic proximal mandible

The lower jaw arises from the mandibular process of the first pharyngeal arch (MdPA1) (Figs. 1A-D). Other derivatives include the malleus, incus (middle ear ossicles) and tympanic ring (Smith and Schneider, 1998). Analysis of bone and cartilage stained E17.5 *Tbx1*$^{-/-}$ embryos shows that the size of the lower jaw is smaller in the *Tbx1*$^{-/-}$ embryos than that of wild-type embryos (Figs. 1A-D), *t* test, p= 0.016 (Fig. S1). The penetrance of malformations is 100% and the type of mandibular phenotype is similar among null mutants. The mutant mandibles are also missing the coronoid process and have a hypoplastic angular process (Figs. 1B, 1D). The proximal part of the mandibular process also gives rise to the tympanic ring and the malleus. The tympanic ring is absent in the *Tbx1*$^{-/-}$ (Fig. 1F) embryos compared to *Tbx1*$^{+/+}$ (Fig. 1E). The malleus, incus and stapes (stapes is derived from the second pharyngeal arch) can be detected in histological tissue sections (Fig. 1G). The malleus is present, but the incus and stapes are missing from *Tbx1*$^{-/-}$ embryos (Fig 1H; Fig. S2). This is similar to what was previously reported (Moraes et al., 2005). Loss of the stapes is not surprising because the second pharyngeal arch is hypoplastic or missing in the mutant embryos. The mandibular arch derived defects are consistent with what has been described earlier in a different *Tbx1* mutant allele (Jerome and Papaioannou, 2001). It has been shown that the maxillary incisors are missing or malformed in the *Tbx1* mutant embryos (Jerome and Papaioannou, 2001). Histological analysis at E17.5 revealed no difference in the structure of mandibular molars (Figs. 1I, IJ) and the incisors (Figs. 1K, 1L). However, there are teeth defects that can be appreciated by taking other approaches. Culture of embryonic teeth showed lack of enamel due to defects of ameloblast lineage in *Tbx1*$^{-/-}$ embryos (Caton et al., 2009; Mitsiadis et al., 2008). *Tbx1* therefore has major roles in development of the mandibular arch skeletal structures. These structures derive from the cranial neural crest cell (NCC) mesenchyme or pharyngeal arch ectoderm (enamel).

Cranial neural crest migration to MdPA1 in *Tbx1*$^{-/-}$ mutant embryos

During craniofacial development, neural crest cells (NCCs) delaminate from the dorsal neural tube and migrate into the pharyngeal arches (Santagati and Rijli, 2003). Lineage tracing studies using a *Wnt1-Cre* transgene and the *ROSA26* conditional reporter (*R26R*) mouse line have confirmed that cranial NCCs differentiate into cartilage and bone, cranial ganglia, teeth and connective tissue of the face and neck (Chai et al., 2000). Many of these

are malformed when *Tbx1* is inactivated. Previous studies of *Tbx1*$^{-/-}$ embryos, using molecular markers, has shown that NCCs are abnormally distributed in the caudal pharyngeal region (Vitelli et al., 2002). Using the *Wnt1-Cre* reporter system (Danielian et al., 1998) (Soriano, 1999), we found no differences at E8.75 for NCCs migration (Figs. 2A, B), but did detect differences at E9.5 (Figs. 2C, D) and E10.5 (Figs. 2E, F). The homeodomain containing gene, *Hoxa2* is required for development of the second pharyngeal arch (PA2; (Rijli et al., 1993). It is robustly expressed in PA2 in wild-type embryos (Fig. 2K) but its expression is reduced in the hypoplastic PA2 (Fig. 2L) or ectopically located in the MdPA1 of *Tbx1*$^{-/-}$ mutants when PA2 is missing (Fig. 2M) consistent with previous findings at E10.5 (Moraes et al., 2005). As anticipated, the *Tbx1*$^{-/-}$ embryos had an additional stream of NCCs migrating into MdPA1 from rhombomere 4 (Fig.2D, arrow), although its exact contribution at E10.5 is small (Figs. 2L-M). In conclusion, while *Tbx1* is not required for the presence of NCCs in MdPA1 (Figs. 2G-J), it is needed for migration of NCCs to the rest of the pharyngeal apparatus. Despite the fact that it makes up the minority of NCCs in MdPA1, it is possible that the ectopic NCCs from PA2 affect patterning. If this is the case, NCC markers should show abnormal expression, especially in the aboral part of the arch. We found that expression patterns of NCC markers *AP2 alpha*, *Sox9*, *Dlx1* and *Dlx2* are similar in wild-type and *Tbx1*$^{-/-}$ embryos at E9.5 and E10.5 (Fig. S3). This suggests some NCC plasticity in adopting MdPA1 fates, despite presence of some NCCs destined to caudal tissues.

β-galactosidase labeled cells was seen in the mesenchyme surrounding the unstained core mesoderm indicating that the core mesoderm (unstained cells; Figs. 2G, H, I, J) is still present in *Tbx1*$^{-/-}$ mutants (Figs. 2H, J). Defects observed in mutants are thus not caused by loss of core mesoderm.

Tbx1 is not required cell autonomously in the NCCs for craniofacial development

Although grossly, it did not appear that *Tbx1* was expressed in the NCCs, it is still possible that a localized domain of expression important for lower jaw development could have been missed. To test this, *Tbx1*$^{flox/flox}$ mice were crossed with the *Wnt1-Cre; Tbx1*$^{+/-}$ mice to generate embryos with *Tbx1* deleted specifically in the NCCs (NCC-KO). Histological sections of the *Wnt1- Cre; Tbx1*$^{flox/-}$ embryos at E17.5 showed that the mandible was equivalent in size (Fig. 3B) when compared with the control (*Wnt1-Cre; Tbx1*$^{flox/+}$; *Control*) embryos (Fig. 3A). Structures that develop from the proximal part of the mandibular process of the first branchial arch; like the incus and tympanic ring; which are missing in the *Tbx1* homozygous mutant embryos were present in the *Wnt1-Cre; Tbx1*$^{flox/-}$ embryos (Figs. 3D and 3F) as compared with control embryos (Figs. 3C and 3E). Mandibular molars (Fig. 3H) and the incisors (Fig. 3J) also formed normally in these embryos when compared with control embryos (Figs. 3G and 3I). *Tbx1* homozygous mutant embryos have a cleft palate (Liao et al., 2004). Analysis of the *Wnt1-Cre; Tbx1*$^{flox/-}$ embryos showed that the palate developed normally in these embryos (Fig. 3L) compared to control (Fig. 3K). The muscles of mastication, including the masseter were missing in *Tbx1*$^{-/-}$ embryos (Liao et al., 2004). However, the masseter muscle was present in the *Wnt1-Cre; Tbx1*$^{flox/-}$ embryos (Fig. 3N), similar to control embryos (Fig. 3M). The absence of craniofacial anomalies in mice, harboring a *Tbx1* deletion in NCCs, demonstrates a non-autonomous role for *Tbx1* in NCCs during mandibular development.

Tbx1 is required to pattern neural crest derived mesenchyme in the mandibular arch

Previous work showed expanded expression of some genes in MdPA1 in *Tbx1*$^{-/-}$ mutants at E10.5 (Kelly et al., 2004). This could explain abnormalities later in development. To follow up, we examined expression of genes important for patterning MdPA1. The orientation of MdPA1 is established when oral (teeth) and aboral domains are formed, rostrally and

caudally, respectively. *Lhx6/8* and *Goosecoid* (*Gsc*) homeobox genes establish the oral-aboral patterning of the lower jaw (Liodis et al., 2007; Rivera-Perez et al., 1995; Tucker et al., 1999; Yamada et al., 1995; Zhao et al., 1999). *Ptx1* gene deleted mice exhibit micrognathia and an abnormal tympanic ring (Lanctot et al., 1999).

The distribution of transcripts for *Lhx6*, *Lhx8* and *Ptx1* in MdPA1 in *Tbx1*$^{-/-}$ embryos was shifted proximally and dorsally as compared to wild-type littermates (Figs. 4A- F'). This was consistent among embryos, despite some inter-embryo differences in overall arch structure within genotypes. A cartoon next to the figure depicts the pattern changes. *Gsc* is expressed in the caudal aboral mesenchyme of the mandibular arch (Figs. 4G, G') (Tucker et al., 1999). Unlike the three, its expression was unaltered (Figs. 4H, H'). The results presented here show that *Tbx1* is required to pattern the NCC derived mesenchyme in specific aspects, but not by globally changing the oral-aboral axes. The ectopic *Hoxa2* expression (Fig. 2M) is in the region of the unchanged *Gsc* expression, supporting the idea that ectopic PA2 NCCs do not influence global NCC gene expression changes.

Genes downstream of Fgf signaling are expanded in the *Tbx1*$^{-/-}$ mandibular arch

As shown above, selected genes were shifted into the proximal part of the arch (proximal of MdPA1 is lateral with respect to the embryo) and expanded dorsally, towards the neural tube in the *Tbx1*$^{-/-}$ mutants. There are four separate pieces of evidence to support the conclusion that fibroblast growth factor (Fgf) signaling acts upstream of the genes (Figure 4, Model). Firstly, they are expressed in the mesenchyme directly beneath an *Fgf8* expressing oral epithelium (Lanctot et al., 1999;Tucker et al., 1999). Secondly, the epithelium is required for the mesenchymal induction of expression of these genes (Bobola et al., 2003;Grigoriou et al., 1998). Furthermore, addition of Fgf- soaked beads mimics this induction (Bobola et al., 2003;Grigoriou et al., 1998). Finally, genetic evidence shows that *Fgf8* is absolutely required for the mesenchymal induction of these genes (Bobola et al., 2003;Trumpp et al., 1999). Since Fgf signaling seems to be the common feature of the induction of *Lhx6*, *Lhx8* and *Ptx1*; we evaluated the expression of *Fgf8* as well as *Spry1*, *Spry2* and *Erm* genes (de Maximy et al., 1999;Minowada et al., 1999;Monte et al., 1994;Raible and Brand, 2001) downstream of Fgf signaling in MdPA1 in wild-type and *Tbx1*$^{-/-}$ embryos. Expression of *Fgf8*, *Spry1*, *Spry2* and *Erm* showed a shift of expression into the proximal (lateral to embryo) and also dorsal region of the mandibular arch in mutant embryos (Fig. 5). Results suggested that Fgf signaling might be altered as well (Fig. 5, Model). Although the shift of *Fgf8* and *Ptx1* expression is very subtle, it can more easily be appreciated in tissue sections (Figs. 6A-F). Additional lateral views of whole mount in situ analysis of *Fgf8* and *Ptx1* are shown for comparison (Figs. 6G-J). These observations suggest that *Tbx1* regulates the precise spatial position of *Fgf8* and its downstream effector genes. If *Fgf8* is shifted in expression, perhaps *Bmp4* is shifted as well.

Bmp4 and downstream gene, *Alx4* are expanded proximally in the *Tbx1*$^{-/-}$ mandibular arch

It is known that *Bmp4* can repress *Fgf8* expression as well as antagonize *Fgf8* signaling. When Noggin beads block *Bmp* signaling in the distal ectoderm, the domain of *Fgf8* expression expands from the proximal region into the distal region, towards the embryo midline (Stottmann et al., 2001). Also, when *Bmp4* is deleted in the mandibular ectoderm, *Fgf8* is expressed in the distal (midline) ectoderm (Liu et al., 2005). Therefore, expression of *Bmp4* was evaluated in the mandibular arches of the *Tbx1* mutant embryos.

Whole mount *in situ* hybridization at E10.5 shows that *Bmp4* is expressed in the distal oral ectoderm of the mandibular arch in wild-type embryos (Figs. 7A, C, E). In the *Tbx1*$^{-/-}$ embryos, the domain of *Bmp4* expression expanded from the distal region into the proximal region (Figs. 7B, D, F). This was also validated by *in situ* hybridization on tissue sections

(Figs. 7G, H, I). We observed loss of *Bmp4* in the most distal ectoderm in some mutants but it was clearly present caudally in MdPA1 (Figs. 7H, I). *Alx4* is a member of the *Aristaless-like* homeobox gene family that is characterized by the presence of a paired- type homeobox and a small, conserved C- terminal domain in the proteins encoded (Meijlink et al., 1999). Mice harboring mutations in *Alx3/Alx4* have severe craniofacial anomalies (Beverdam et al., 2001). *Alx4* is proposed to be a target of Bmp signaling (Rice et al., 2003; Selever et al., 2004). Its expression is lost in the mandibular mesenchyme of oral ectoderm deleted *Bmp4* mice (Liu et al., 2005). *Alx4*, normally expressed in the distal mesenchyme (Figs. 7J, L, N, P, R) was shifted proximally in the mesenchyme of the *Tbx1* null mutant embryos (Figs. 7K, M, O, Q, S, T). These results suggest that *Tbx1* restricts the precise spatial position of *Bmp4* and its downstream signaling target, *Alx4* in the mandibular ectoderm and NCC mesenchyme, respectively. Thus it is possible that Tbx1 directly or indirectly restricts expression of either *Fgf8* and/or *Bmp4* in the oral ectoderm.

Mesodermal *Tbx1* regulates mandibular patterning

To investigate whether *Tbx1* could regulate the expression of *Bmp4* and *Fgf8* in a cell-autonomous manner, we evaluated the expression of *Tbx1* at different stages of development. At all stages examined, from E8.5 to E10.5, we did not see expression of *Tbx1* in the mandibular ectoderm (Figs. 8A-C). At E8.5, expression of *Tbx1* is seen in the mesoderm of the first pharyngeal arch (Fig. 8A). Expression is also seen in the caudal pharyngeal ectoderm (Fig. 8A). At E9.5, *Tbx1* is expressed in the core mesoderm of the first pharyngeal arch and in the first pharyngeal pouch endoderm (Fig. 8B). We previously showed that the mandible is similarly hypoplastic by inactivating *Tbx1* using the *Foxg1-Cre* endodermal driver (Arnold et al., 2006); Fig. S4). However, there is strong evidence that *Tbx1* has independent functions in the mesoderm (Braunstein et al., 2009; Zhang et al., 2006). Whole mount *in situ* hybridization at E10.5 revealed expression of *Tbx1* in the core mandibular mesoderm (Fig. 8C). Note that the core mesodermal domain of *Tbx1* expression occupies the proximal corner of MdPA1 where later jaw defects occur (Fig. 8C). The absence of expression of *Tbx1* in the mandibular ectoderm suggests a non-autonomous role for *Tbx1* during mandibular development.

To delineate the role of mesodermal *Tbx1* in mandibular development, we examined bone and cartilage stained E17.5, *T- Cre; Tbx1*$^{flox/-}$ embryos (Fig. 8E). *T- Cre; Tbx1*$^{flox/-}$ (*TKO*) embryos have been previously described (Braunstein et al., 2009;Liao et al., 2008), where *Tbx1* is conditionally ablated only in its mesodermal domains of expression. Our analysis shows that 60% (6 out of 10) of the *TKO* mandibles (Fig. 8E) were smaller than the wild-type mandibles (Fig. 8D). They also had a missing coronoid process and a hypoplastic angular process, thus recapitulating the *Tbx1*$^{-/-}$ phenotype (Fig. 8F). About 40% (4 out of 10) of the *TKO* mandibles were like the wild-type ones (data not shown). Reduced penetrance is not surprising considering the hypomorphic nature of the allele in our mutants (Liao et al., 2008). Specifically, we found residual *Tbx1* expression in *T-Cre* or *Mesp1-Cre* mediated *Tbx1* conditional null mutant embryos. Nonetheless, phenotypes were consistent. To make sure we have examined sufficient mutant embryos, in the case of phenotypes with reduced penetrance, we examined double the amount that would be needed if there were a completely invariant phenotype. The malleus was present in *TKO* mutants (n = 12 ears), the incus was present in two ears, while the stapes was absent, perhaps secondary to the hypoplastic nature or loss of the second pharyngeal arch (Fig. S2).

We also evaluated the expression of *Fgf8* and *Bmp4* in the *TKO* embryos at E10.5. Whole mount *in situ* hybridization shows that the expression of *Fgf8* (and *Spry2, Ptx1*) was shifted proximally in the mutant mandibular arches (Fig. 8G) as compared with wild-type, similar to that observed in *Tbx1*$^{-/-}$ embryos, but with reduced penetrance. Four out of six (66.6%) mandibular arches examined show the proximal expansion of the distally expressed *Bmp4*

and *Alx4* in the TKO embryos as compared to wild-type (Fig. 8G). Two out of six (23.4%) of the mandibular arches of the *TKO* mutants looked like the wild-type embryos. This can again be attributed to the hypomorphic nature of the *TKO* embryos (Liao et al., 2008). These results suggest that mesodermal *Tbx1* shapes the mandibular arch, independent of endodermal *Tbx1*, which is also required (Arnold et al., 2006). Since *Tbx1* is required separately in two independent tissues, endoderm and mesoderm, it is possible that they affect similar signaling pathways. *Hoxa2* expression was examined in *TKO* mutants and as expected, there was variability in expression pattern in MdPA1 and PA2 depending upon the severity of the phenotype (Fig. 8H). In embryos with a PA2 present, expression was normal. In embryos where PA2 was hypoplastic or missing, ectopic *Hoxa2* expression was noted in MdPA1, as in *Tbx1* null mutants (Fig. 8H).

Role of Shh signaling in patterning MdPA1

Shh (Sonic hedgehog) is a secreted morphogen expressed in the pharyngeal endoderm and it is required to pattern the craniofacial region. Its loss leads to a severe craniofacial disorder termed holoprosencephaly and it includes loss of first arch derivatives (Cordero et al., 2004; Lazaro et al., 2004; Nagase et al., 2005). *Shh* is expressed in the pharyngeal endoderm that abuts against the ectoderm (ten Berge et al., 2001) but it is not directly overlapping with *Fgf8* expression, at least in chick (Haworth et al., 2007). *Shh* is required for survival of first arch cranial NCCs (Ahlgren and Bronner-Fraser, 1999; Moore-Scott and Manley, 2005; Yamagishi et al., 2006). It promotes *Fgf8* and *Bmp4* expression in the mandibular ectoderm in the chick (Brito et al., 2008; Haworth et al., 2007). Shh mediated signaling is thought to act upstream of *Tbx1* in the pharyngeal endoderm and mesoderm (Garg et al., 2001). To determine if *Tbx1* might provide feedback on the *Shh* pathway, we examined expression of *Shh* downstream of *Tbx1* and there were no significant differences in the $Tbx1^{-/-}$ mutant embryos (Fig. 9). However, subtle changes could have occurred. Patched (*Ptch1*) is the cell surface receptor for Shh ligand, and is upregulated in *Shh* responsive tissues (Hahn et al., 1996). *Ptch1* is a downstream effector gene of *Shh* (Haraguchi et al., 2001; Hardcastle et al., 1998). To determine if there were subtle changes in *Shh* signaling beyond the resolution of the *in situ* sections, we examined *Ptch1* expression. *Ptch1* expression was present in the proximal MdPA1 but diminished in the distal MdPA1 mesenchyme in $Tbx1^{-/-}$ mutant embryos at E10.5 (Figure 9). This might explain why *Bmp4* expression is reduced in the distal ectoderm of MdPA1.

Endothelin, dHAND and *eHAND* pathways

Endothelin-1 (Edn1) encodes a secreted peptide, ET-1 from the pharyngeal ectoderm which forms a gradient in the NCC mesenchyme to form skeletal derivatives of the first arch (Thomas et al., 1998; Yanagisawa et al., 2003). ET-1 stimulates expression of the basic helix-loop-helix (bHLH) transcription factor gene, *dHAND*, in the NCC mesenchyme of the first arch (Thomas et al., 1998; Yanagisawa et al., 2003). Inactivation of *Edn1* results in a phenocopy of VCFS/DGS (Thomas et al., 1998) and the $Tbx1^{-/-}$ mutation. Both *dHAND* as well as *eHAND* transcripts were expressed relatively normally in the midline in $Tbx1^{-/-}$ mutants at E10.5 (Fig. S5). There was a very slight expansion of *dHAND* in the aboral border of MdPA1. It is not clear whether this change could have resulted in phenotypic changes observed. It is possible that changes in cell proliferation or survival might contribute to changes in gene expression observed.

No detectable changes in cell proliferation or apoptosis in the MdPA1 at E10.5

It seems reasonable to speculate that a proximal shift of signaling molecules could be caused by changes in MdPA1 shape. This could result from alteration of cell proliferation or apoptosis. The extent of proliferation in the mandibular arch was extensive in $Tbx1^{-/-}$ and wildtype embryos at E10.5. Within the arch, however, zones with high localized

proliferation in the NCC mesenchyme were identified in the periphery (Figs. 10A, A'). There were no significant differences in number of proliferating cells between different genotypes at this stage. Apoptosis was concentrated in the rostral midline (Figs. 10B, B'). There were no changes in apoptosis either (Fig. 10, Table). Thus, at this stage, where significant shift in *Fgf8* and *Bmp4* expression and that of some of their effector genes occurred, there were no major changes in cell proliferation or survival, rather cell fate changes might be responsible.

To understand whether mandibular defects are secondary to failed formation of the masseter muscle, E17.5 histological sections were examined. The masseter was absent in *Tbx1*$^{-/-}$ embryos (Fig. S6). It was absent in mutants in which *Tbx1* was inactivated using the *Foxg1-Cre* driver, although the mandible had similar defects as the null mutant (Arnold et al., 2006). In contrast, the masseter was present in all *TKO* mutant embryos (n= 7; Fig. S6) indicating that the mandiblular defect is not dependent on loss of the masseter in the *Tbx1* null and tissue specific mutants.

DISCUSSION

Lower jaw skeletal elements derived from the proximal mandibular arch are missing or abnormal when *Tbx1* is inactivated. In this report, we show that this corresponds to a shift in gene expression in the region of the mandible that is malformed when the axes are being established. Signaling interplay between the various tissues that make up the mandibular process of the first arch is crucial for its development. Experimental data suggest an instructive role for epithelial tissues in patterning, outgrowth and morphogenesis of the mandibular processes. Classical tissue recombination studies have demonstrated that the epithelium is required for outgrowth and correct skeletogenesis in the mandibular arch to form the proximal jaw (Mina, 2001). Conditional inactivation of *Fgf8* signaling in the pharyngeal ectoderm resulted in the disappearance of the proximal portion of the mandible (Trumpp et al., 1999), thus supporting the critical function of ectodermal *Fgf* signaling. Conditional deletion of *Bmp4* in the mandibular ectoderm and to a lesser extent in the endoderm, results in severe defects in mandibular development (Liu et al., 2005). Craniofacial ectoderm also regulates the expression of transcription factors to specify the fate of cranial neural crest cells (NCCs) forming the lower jaw (Tucker et al., 1999).

It has been demonstrated that the endoderm has a similar patterning role during morphogenesis of the lower jaw skeleton. Specific grafted portions of chick endodermal tissue can induce formation of supernumerary jaw elements. This can also determine their position and orientation (Couly et al., 2002). Loss of endoderm results in the absence of *Fgf8* expression in the first pharyngeal arch ectoderm (Haworth et al., 2004). In the zebrafish mutant *Casanova* which has endoderm defects, pharyngeal arch cartilages are defective (David et al., 2002). This provides evidence that the endoderm is important for patterning the pharyngeal arch skeleton. Thus, it is clear that endodermal mediated signaling plays important roles in determining the patterning of the mandibular arch to form the complex skeletal structure of the lower jaw. Inactivation of *Tbx1* in the pharyngeal endoderm using a *Foxg1-Cre* driver resulted in a hypoplastic lower jaw (Arnold et al., 2006) (Supplement Fig.3). *Fgf8* is expressed in the endoderm downstream of *Tbx1* (Arnold et al., 2006), suggesting that alteration of Fgf8 signaling to surrounding mdPA1 tissues may perturb its development.

In addition to the endoderm, NCCs themselves might provide important signals for patterning. The first pharyngeal arch NCCs are devoid of *Hox* gene expression. Using quail-duck interspecies grafting, it has been shown that donor NCCs provide patterning instructions for beak morphology within the host environment (Schneider and Helms, 2003);

indicating that NCCs carry some independent morphogenetic information. The gene, *Hoxa2* is strongly expressed in the second pharyngeal arch. Interestingly, it was shown that signals (as yet to be delineated) from the mesoderm influence *Hox* gene expression in NCCs in the second pharyngeal arch by culturing mouse embryos (Trainor and Krumlauf, 2000b).

Our study shows that the pharyngeal arch core mesoderm has an indirect but important role in shaping the proximal portion of the lower jaw. Spatial relationship between *Bmp4* distally and *Fgf8* in the proximal ectoderm pre-patterns the jaw axis. However, it largely remains unknown as to how these spatially restricted patterns of expression are established and regulated. Our study sheds key new light into this process. Here we show that *Fgf8* and *Bmp4* spatial domains in the ectoderm, as well as that of their downstream genes in the NCCs as shown in the model in Figure 11, are altered in *Tbx1* null and mesodermal conditional *Tbx1* null mutants, implicating the mesoderm as a key player in shaping the proximal lower jaw. In this figure we show that *Tbx1* might serve to repress gene expression in the proximal MdPA1 ectoderm (*Bmp4* and *Fgf8*). In the Model, Bmp4 and Fgf8 signaling molecules in the ectoderm modulate expression of NCC specific genes, cell non-autonomously. Neither is expressed in the core pharyngeal mesoderm. What genes could Tbx1 regulate in the mesoderm that could signal to the surrounding ectoderm? Very few studies have shown a role of the core mesoderm in patterning the pharyngeal arches. The mesoderm was considered important for formation of craniofacial muscles, but not as a signaling center. In this report, we suggest that the mesoderm may have a role in cell fate changes resulting in mandible structural defects and loss of the incus (middle ear bone).

There are several important soluble morphogens expressed in the core mesoderm of MdPA1. One gene is *Fgf10*, which is expressed in MdPA1, and diminished in $Tbx1^{-/-}$ mutant embryos (Vitelli et al., 2002). Tbx1 is able to activate the *Fgf10* promoter in cell culture (Xu et al., 2004). $Fgf10^{-/-}$ mice have cleft palate (Alappat et al., 2005), however the lower jaw appeared to be normal (Hajihosseini et al., 2009). It is possible that other Fgf ligands provide a redundant function in shaping the lower jaw with *Fgf10* by regulating expression of *Sprouty* genes in the NCCs, that will in turn, limit expression of *Fgf8* in the ectoderm prior to E10.5. Similarly, Bmp antagonists secreted from the core mesoderm might restrict expression of *Bmp4* in the proximal ectoderm. Tbx1 might regulate Bmp antagonists, and when inactivated prior to the changes observed at E10.5, result in expansion of the *Bmp4* domain. Of interest, a soluble Bmp antagonist, *Chordin-like 1* (*Chrdl1*; aka *Neuralin 1*) is expressed strongly in the pharyngeal core mesoderm (Coffinier et al., 2001). It is possible that it might be downstream of *Tbx1* and thus, its loss would promote shifting of gene expression observed in the mutant embryos. In order to fully understand signaling from the mesoderm it will be necessary to take unbiased genome wide approaches in conditional mutants to discover genes and then to eventually characterize signaling pathways downstream. We examined expression of *Shh* in the oral endoderm, lying adjacent to ectodermal *Bmp4* and *Fgf8*. Although its expression appeared unchanged in the null mutants, its receptor, *Ptch1*, was downregulated in the distal MdPA1, suggesting subtle changes in Shh signaling. More work needs to be done to examine the *Shh* pathway members more closely to determine if any are co-expressed in the core mesoderm with *Tbx1*.

Alternatively, it is possible that *Tbx1* is essential for normal migration of NCCs from the rhombomeres to the arches. Abnormal migration of second pharyngeal arch NCCs into the mandibular arch when *Tbx1* is inactivated can alter the local environment resulting in the abnormalities observed (Moraes et al., 2005; Vitelli et al., 2002). A small pocket of *Hoxa2* positive cells is ectopically located in conditional and null mutants. There is evidence supporting and negating NCC plasticity coming from the rhombomeres to fill the pharyngeal arches. Whether Hox^{+} NCCs are able or unable to respond to local cues and change fate

according to their environment has been studied and remains unsolved in part because plasticity might be temporally dependent. Studies in chick and mice have shown some plasticity in NCCs, depending on stage of development (Santagati and Rijli, 2003; Trainor and Krumlauf, 2000a; Trainor and Krumlauf, 2000b). One issue that cannot be ruled out is whether morphology defects due to a small or missing second arch (and ectopic NCCs in MdPA1) influence patterning independent to signaling within MdPA1 from mesodermal *Tbx1* and downstream genes. More work will need to be done to evaluate these questions in the future with MdPA1 specific mouse knockouts.

In summary, we found that *Tbx1* has a role in the paraxial core mesoderm in shaping the proximal mandible. Thus, *Tbx1* is required both in the pharyngeal endoderm (Arnold et al., 2006) and mesoderm to pattern the lower jaw, cell non-autonomously. Similar to inner ear and cardiac outflow tract development, *Tbx1* is required independently in each tissue where it is expressed (Arnold et al., 2006; Braunstein et al., 2009; Xu et al., 2004; Zhang et al., 2005; Zhang et al., 2006). To understand the molecular pathway, we took a candidate gene approach and found specific alteration of expression of ectodermal *Fgf8* and *Bmp4* and a subset of downstream effector genes in NCCs, in the region of the MdPA1 in *Tbx1*$^{-/-}$ embryos that will form the proximal mandible. Similar findings were obtained when *Tbx1* was downregulated in the core mesoderm. This demonstrates new functions for the core paraxial mesoderm in interacting with surrounding tissues to help shape complex skeletal structures.

Supplementary Material

Refer to Web version on PubMed Central for supplementary material.

Acknowledgments

We thank Dr. Radma Mahmood for technical assistance; Dr. Mark Lewandoski for *T-Cre* transgenic mouse strain; Dr. John Hebert, Dr. Malcolm Logan, Dr. Hubert Schorle, Dr. Gail Martin, Dr. Karine Rizzoti and Dr. Frits Meijlink for probes. This work was supported by NIH grant 1R01HL088698 (B.E.M.).

References

Ahlgren SC, Bronner-Fraser M. Inhibition of sonic hedgehog signaling in vivo results in craniofacial neural crest cell death. Curr Biol. 1999; 9:1304–1314. [PubMed: 10574760]

Alappat SR, Zhang Z, Suzuki K, Zhang X, Liu H, Jiang R, Yamada G, Chen Y. The cellular and molecular etiology of the cleft secondary palate in Fgf10 mutant mice. Dev Biol. 2005; 277:102–113. [PubMed: 15572143]

Arnold JS, Werling U, Braunstein EM, Liao J, Nowotschin S, Edelmann W, Hebert JM, Morrow BE. Inactivation of Tbx1 in the pharyngeal endoderm results in 22q11DS malformations. Development. 2006; 133:977–987. [PubMed: 16452092]

Beresford WA. Schemes of zonation in the mandibular condyle. Am J Orthod. 1975; 68:189–195. [PubMed: 1056706]

Beverdam A, Brouwer A, Reijnen M, Korving J, Meijlink F. Severe nasal clefting and abnormal embryonic apoptosis in Alx3/Alx4 double mutant mice. Development. 2001; 128:3975–3986. [PubMed: 11641221]

Bobola N, Carapuco M, Ohnemus S, Kanzler B, Leibbrandt A, Neubuser A, Drouin J, Mallo M. Mesenchymal patterning by Hoxa2 requires blocking Fgf-dependent activation of Ptx1. Development. 2003; 130:3403–3414. [PubMed: 12810588]

Braunstein EM, Monks DC, Aggarwal VS, Arnold JS, Morrow BE. Tbx1 and Brn4 regulate retinoic acid metabolic genes during cochlear morphogenesis. BMC Dev Biol. 2009; 9:31. [PubMed: 19476657]

Brito JM, Teillet MA, Le Douarin NM. Induction of mirror-image supernumerary jaws in chicken mandibular mesenchyme by Sonic Hedgehog-producing cells. Development. 2008; 135:2311–2319. [PubMed: 18539924]

Butts SC. The facial phenotype of the velo-cardio-facial syndrome. Int J Pediatr Otorhinolaryngol. 2009; 73:343–350. [PubMed: 19062108]

Caton J, Luder HU, Zoupa M, Bradman M, Bluteau G, Tucker AS, Klein O, Mitsiadis TA. Enamel-free teeth: Tbx1 deletion affects amelogenesis in rodent incisors. Dev Biol. 2009; 328:493–505. [PubMed: 19233155]

Chai Y, Jiang X, Ito Y, Bringas P Jr. Han J, Rowitch DH, Soriano P, McMahon AP, Sucov HM. Fate of the mammalian cranial neural crest during tooth and mandibular morphogenesis. Development. 2000; 127:1671–1679. [PubMed: 10725243]

Coffinier C, Tran U, Larrain J, De Robertis EM. Neuralin-1 is a novel Chordin-related molecule expressed in the mouse neural plate. Mech Dev. 2001; 100:119–122. [PubMed: 11118896]

Cordero D, Marcucio R, Hu D, Gaffield W, Tapadia M, Helms JA. Temporal perturbations in sonic hedgehog signaling elicit the spectrum of holoprosencephaly phenotypes. J Clin Invest. 2004; 114:485–494. [PubMed: 15314685]

Couly G, Creuzet S, Bennaceur S, Vincent C, Le Douarin NM. Interactions between Hox-negative cephalic neural crest cells and the foregut endoderm in patterning the facial skeleton in the vertebrate head. Development. 2002; 129:1061–1073. [PubMed: 11861488]

Danielian PS, Muccino D, Rowitch DH, Michael SK, McMahon AP. Modification of gene activity in mouse embryos in utero by a tamoxifen-inducible form of Cre recombinase. Curr Biol. 1998; 8:1323–1326. [PubMed: 9843687]

David NB, Saint-Etienne L, Tsang M, Schilling TF, Rosa FM. Requirement for endoderm and FGF3 in ventral head skeleton formation. Development. 2002; 129:4457–4468. [PubMed: 12223404]

de Maximy AA, Nakatake Y, Moncada S, Itoh N, Thiery JP, Bellusci S. Cloning and expression pattern of a mouse homologue of drosophila sprouty in the mouse embryo. Mech Dev. 1999; 81:213–216. [PubMed: 10330503]

Garg V, Yamagishi C, Hu T, Kathiriya IS, Yamagishi H, Srivastava D. Tbx1, a DiGeorge syndrome candidate gene, is regulated by sonic hedgehog during pharyngeal arch development. Dev Biol. 2001; 235:62–73. [PubMed: 11412027]

Graham A. Development of the pharyngeal arches. Am J Med Genet A. 2003; 119A:251–256. [PubMed: 12784288]

Grigoriou M, Tucker AS, Sharpe PT, Pachnis V. Expression and regulation of Lhx6 and Lhx7, a novel subfamily of LIM homeodomain encoding genes, suggests a role in mammalian head development. Development. 1998; 125:2063–2074. [PubMed: 9570771]

Hahn H, Christiansen J, Wicking C, Zaphiropoulos PG, Chidambaram A, Gerrard B, Vorechovsky I, Bale AE, Toftgard R, Dean M, Wainwright B. A mammalian patched homolog is expressed in target tissues of sonic hedgehog and maps to a region associated with developmental abnormalities. J Biol Chem. 1996; 271:12125–12128. [PubMed: 8647801]

Hajihosseini MK, Duarte R, Pegrum J, Donjacour A, Lana-Elola E, Rice DP, Sharpe J, Dickson C. Evidence that Fgf10 contributes to the skeletal and visceral defects of an Apert syndrome mouse model. Dev Dyn. 2009; 238:376–385. [PubMed: 18773495]

Hall BK. Tissue interactions and the initiation of osteogenesis and chondrogenesis in the neural crest-derived mandibular skeleton of the embryonic mouse as seen in isolated murine tissues and in recombinations of murine and avian tissues. J Embryol Exp Morphol. 1980; 58:251–264. [PubMed: 7441157]

Haraguchi R, Mo R, Hui C, Motoyama J, Makino S, Shiroishi T, Gaffield W, Yamada G. Unique functions of Sonic hedgehog signaling during external genitalia development. Development. 2001; 128:4241–4250. [PubMed: 11684660]

Hardcastle Z, Mo R, Hui CC, Sharpe PT. The Shh signalling pathway in tooth development: defects in Gli2 and Gli3 mutants. Development. 1998; 125:2803–2811. [PubMed: 9655803]

Havkin N, Tatum SA, Shprintzen RJ. Velopharyngeal insufficiency and articulation impairment in velo-cardio-facial syndrome: the influence of adenoids on phonemic development. Int J Pediatr Otorhinolaryngol. 2000; 54:103–110. [PubMed: 10967379]

Haworth KE, Healy C, Morgan P, Sharpe PT. Regionalisation of early head ectoderm is regulated by endoderm and prepatterns the orofacial epithelium. Development. 2004; 131:4797–4806. [PubMed: 15342462]

Haworth KE, Wilson JM, Grevellec A, Cobourne MT, Healy C, Helms JA, Sharpe PT, Tucker AS. Sonic hedgehog in the pharyngeal endoderm controls arch pattern via regulation of Fgf8 in head ectoderm. Dev Biol. 2007; 303:244–258. [PubMed: 17187772]

Jerome LA, Papaioannou VE. DiGeorge syndrome phenotype in mice mutant for the T-box gene, Tbx1. Nat Genet. 2001; 27:286–291. [PubMed: 11242110]

Kelly RG, Jerome-Majewska LA, Papaioannou VE. The del22q11.2 candidate gene Tbx1 regulates branchiomeric myogenesis. Hum Mol Genet. 2004; 13:2829–2840. [PubMed: 15385444]

Lanctot C, Moreau A, Chamberland M, Tremblay ML, Drouin J. Hindlimb patterning and mandible development require the Ptx1 gene. Development. 1999; 126:1805–1810. [PubMed: 10101115]

Lazaro L, Dubourg C, Pasquier L, Le Duff F, Blayau M, Durou MR, de la Pintiere AT, Aguilella C, David V, Odent S. Phenotypic and molecular variability of the holoprosencephalic spectrum. Am J Med Genet A. 2004; 129A:21–24. [PubMed: 15266610]

Liao J, Aggarwal VS, Nowotschin S, Bondarev A, Lipner S, Morrow BE. Identification of downstream genetic pathways of Tbx1 in the second heart field. Dev Biol. 2008; 316:524–537. [PubMed: 18328475]

Liao J, Kochilas L, Nowotschin S, Arnold JS, Aggarwal VS, Epstein JA, Brown MC, Adams J, Morrow BE. Full spectrum of malformations in velo-cardio-facial syndrome/DiGeorge syndrome mouse models by altering Tbx1 dosage. Hum Mol Genet. 2004; 13:1577–1585. [PubMed: 15190012]

Lindsay EA, Vitelli F, Su H, Morishima M, Huynh T, Pramparo T, Jurecic V, Ogunrinu G, Sutherland HF, Scambler PJ, Bradley A, Baldini A. Tbx1 haploinsufficieny in the DiGeorge syndrome region causes aortic arch defects in mice. Nature. 2001; 410:97–101. [PubMed: 11242049]

Liodis P, Denaxa M, Grigoriou M, Akufo-Addo C, Yanagawa Y, Pachnis V. Lhx6 activity is required for the normal migration and specification of cortical interneuron subtypes. J Neurosci. 2007; 27:3078–3089. [PubMed: 17376969]

Liu W, Selever J, Murali D, Sun X, Brugger SM, Ma L, Schwartz RJ, Maxson R, Furuta Y, Martin JF. Threshold-specific requirements for Bmp4 in mandibular development. Dev Biol. 2005; 283:282–293. [PubMed: 15936012]

Meijlink F, Beverdam A, Brouwer A, Oosterveen TC, Berge DT. Vertebrate aristaless-related genes. Int J Dev Biol. 1999; 43:651–663. [PubMed: 10668975]

Merscher S, Funke B, Epstein JA, Heyer J, Puech A, Lu MM, Xavier RJ, Demay MB, Russell RG, Factor S, Tokooya K, Jore BS, Lopez M, Pandita RK, Lia M, Carrion D, Xu H, Schorle H, Kobler JB, Scambler P, Wynshaw-Boris A, Skoultchi AI, Morrow BE, Kucherlapati R. TBX1 is responsible for cardiovascular defects in velo-cardio-facial/DiGeorge syndrome. Cell. 2001; 104:619–629. [PubMed: 11239417]

Mina M. Regulation of mandibular growth and morphogenesis. Crit Rev Oral Biol Med. 2001; 12:276–300. [PubMed: 11603502]

Minowada G, Jarvis LA, Chi CL, Neubuser A, Sun X, Hacohen N, Krasnow MA, Martin GR. Vertebrate Sprouty genes are induced by FGF signaling and can cause chondrodysplasia when overexpressed. Development. 1999; 126:4465–4475. [PubMed: 10498682]

Mitsiadis TA, Tucker AS, De Bari C, Cobourne MT, Rice DP. A regulatory relationship between Tbx1 and FGF signaling during tooth morphogenesis and ameloblast lineage determination. Dev Biol. 2008; 320:39–48. [PubMed: 18572158]

Monte D, Baert JL, Defossez PA, de Launoit Y, Stehelin D. Molecular cloning and characterization of human ERM, a new member of the Ets family closely related to mouse PEA3 and ER81 transcription factors. Oncogene. 1994; 9:1397–1406. [PubMed: 8152800]

Moore-Scott BA, Manley NR. Differential expression of Sonic hedgehog along the anterior-posterior axis regulates patterning of pharyngeal pouch endoderm and pharyngeal endoderm-derived organs. Dev Biol. 2005; 278:323–335. [PubMed: 15680353]

Moraes F, Novoa A, Jerome-Majewska LA, Papaioannou VE, Mallo M. Tbx1 is required for proper neural crest migration and to stabilize spatial patterns during middle and inner ear development. Mech Dev. 2005; 122:199–212. [PubMed: 15652707]

Nagase T, Nagase M, Osumi N, Fukuda S, Nakamura S, Ohsaki K, Harii K, Asato H, Yoshimura K. Craniofacial anomalies of the cultured mouse embryo induced by inhibition of sonic hedgehog signaling: an animal model of holoprosencephaly. J Craniofac Surg. 2005; 16:80–88. [PubMed: 15699650]

Nowotschin S, Liao J, Gage PJ, Epstein JA, Campione M, Morrow BE. Tbx1 affects asymmetric cardiac morphogenesis by regulating Pitx2 in the secondary heart field. Development. 2006; 133:1565–1573. [PubMed: 16556915]

Perantoni AO, Timofeeva O, Naillat F, Richman C, Pajni-Underwood S, Wilson C, Vainio S, Dove LF, Lewandoski M. Inactivation of FGF8 in early mesoderm reveals an essential role in kidney development. Development. 2005; 132:3859–3871. [PubMed: 16049111]

Raible F, Brand M. Tight transcriptional control of the ETS domain factors Erm and Pea3 by Fgf signaling during early zebrafish development. Mech Dev. 2001; 107:105–117. [PubMed: 11520667]

Rice R, Rice DP, Olsen BR, Thesleff I. Progression of calvarial bone development requires Foxc1 regulation of Msx2 and Alx4. Dev Biol. 2003; 262:75–87. [PubMed: 14512019]

Rijli FM, Mark M, Lakkaraju S, Dierich A, Dolle P, Chambon P. A homeotic transformation is generated in the rostral branchial region of the head by disruption of Hoxa-2, which acts as a selector gene. Cell. 1993; 75:1333–1349. [PubMed: 7903601]

Rivera-Perez JA, Mallo M, Gendron-Maguire M, Gridley T, Behringer RR. Goosecoid is not an essential component of the mouse gastrula organizer but is required for craniofacial and rib development. Development. 1995; 121:3005–3012. [PubMed: 7555726]

Santagati F, Rijli FM. Cranial neural crest and the building of the vertebrate head. Nat Rev Neurosci. 2003; 4:806–818. [PubMed: 14523380]

Schneider RA, Helms JA. The cellular and molecular origins of beak morphology. Science. 2003; 299:565–568. [PubMed: 12543976]

Selever J, Liu W, Lu MF, Behringer RR, Martin JF. Bmp4 in limb bud mesoderm regulates digit pattern by controlling AER development. Dev Biol. 2004; 276:268–279. [PubMed: 15581864]

Smith KK, Schneider RA. Have gene knockouts caused evolutionary reversals in the mammalian first arch? Bioessays. 1998; 20:245–255. [PubMed: 9631652]

Soriano P. Generalized lacZ expression with the ROSA26 Cre reporter strain. Nat Genet. 1999; 21:70–71. [PubMed: 9916792]

Stottmann RW, Anderson RM, Klingensmith J. The BMP antagonists Chordin and Noggin have essential but redundant roles in mouse mandibular outgrowth. Dev Biol. 2001; 240:457–473. [PubMed: 11784076]

ten Berge D, Brouwer A, Korving J, Reijnen MJ, van Raaij EJ, Verbeek F, Gaffield W, Meijlink F. Prx1 and Prx2 are upstream regulators of sonic hedgehog and control cell proliferation during mandibular arch morphogenesis. Development. 2001; 128:2929–2938. [PubMed: 11532916]

Thomas T, Kurihara H, Yamagishi H, Kurihara Y, Yazaki Y, Olson EN, Srivastava D. A signaling cascade involving endothelin-1, dHAND and msx1 regulates development of neural-crest-derived branchial arch mesenchyme. Development. 1998; 125:3005–3014. [PubMed: 9671575]

Trainor P, Krumlauf R. Plasticity in mouse neural crest cells reveals a new patterning role for cranial mesoderm. Nat Cell Biol. 2000a; 2:96–102. [PubMed: 10655589]

Trainor PA, Krumlauf R. Patterning the cranial neural crest: hindbrain segmentation and Hox gene plasticity. Nat Rev Neurosci. 2000b; 1:116–124. [PubMed: 11252774]

Trumpp A, Depew MJ, Rubenstein JL, Bishop JM, Martin GR. Cre-mediated gene inactivation demonstrates that FGF8 is required for cell survival and patterning of the first branchial arch. Genes Dev. 1999; 13:3136–3148. [PubMed: 10601039]

Tucker AS, Yamada G, Grigoriou M, Pachnis V, Sharpe PT. Fgf-8 determines rostral-caudal polarity in the first branchial arch. Development. 1999; 126:51–61. [PubMed: 9834185]

Vitelli F, Morishima M, Taddei I, Lindsay EA, Baldini A. Tbx1 mutation causes multiple cardiovascular defects and disrupts neural crest and cranial nerve migratory pathways. Hum Mol Genet. 2002; 11:915–922. [PubMed: 11971873]

Xu H, Morishima M, Wylie JN, Schwartz RJ, Bruneau BG, Lindsay EA, Baldini A. Tbx1 has a dual role in the morphogenesis of the cardiac outflow tract. Development. 2004; 131:3217–3227. [PubMed: 15175244]

Yamada G, Mansouri A, Torres M, Stuart ET, Blum M, Schultz M, De Robertis EM, Gruss P. Targeted mutation of the murine goosecoid gene results in craniofacial defects and neonatal death. Development. 1995; 121:2917–2922. [PubMed: 7555718]

Yamagishi C, Yamagishi H, Maeda J, Tsuchihashi T, Ivey K, Hu T, Srivastava D. Sonic hedgehog is essential for first pharyngeal arch development. Pediatr Res. 2006; 59:349–354. [PubMed: 16492970]

Yanagisawa H, Clouthier DE, Richardson JA, Charite J, Olson EN. Targeted deletion of a branchial arch-specific enhancer reveals a role of dHAND in craniofacial development. Development. 2003; 130:1069–1078. [PubMed: 12571099]

Zhang Z, Cerrato F, Xu H, Vitelli F, Morishima M, Vincentz J, Furuta Y, Ma L, Martin JF, Baldini A, Lindsay E. Tbx1 expression in pharyngeal epithelia is necessary for pharyngeal arch artery development. Development. 2005; 132:5307–5315. [PubMed: 16284121]

Zhang Z, Huynh T, Baldini A. Mesodermal expression of Tbx1 is necessary and sufficient for pharyngeal arch and cardiac outflow tract development. Development. 2006; 133:3587–3595. [PubMed: 16914493]

Zhao Y, Guo YJ, Tomac AC, Taylor NR, Grinberg A, Lee EJ, Huang S, Westphal H. Isolated cleft palate in mice with a targeted mutation of the LIM homeobox gene lhx8. Proc Natl Acad Sci U S A. 1999; 96:15002–15006. [PubMed: 10611327]

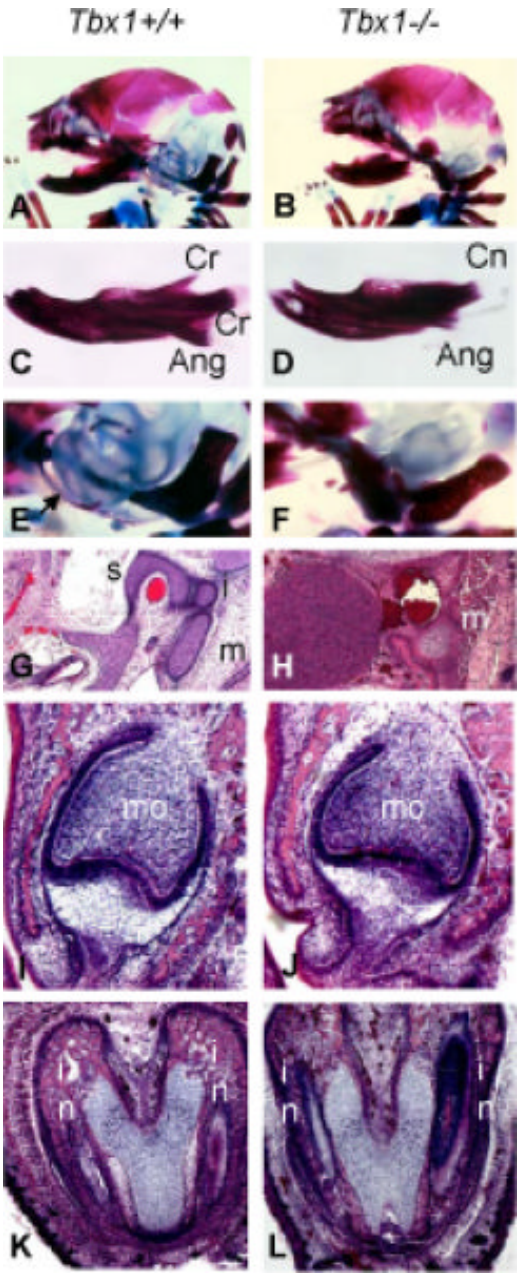

FIGURE 1. Mandibular skeletal phenotype in *Tbx1*$^{-/-}$ embryos

(A-F) Skeletal preparations of E17.5 dpc embryos showing ossified areas in red and cartilage in blue. (A, B) Lateral view of head of wild-type *Tbx1*$^{+/+}$ (A) and *Tbx1*$^{-/-}$ (B) embryo (see Fig. S1). (C, D) Mandible of a wild-type embryo (C) and a *Tbx1*$^{-/-}$ embryo (D). Cr, coronoid process; Cn, condylar process; Ang, angular process. (E, F) Ear capsule of *Tbx1*$^{+/+}$ (E) and *Tbx1*$^{-/-}$ (G) embryo. Arrow denotes the tympanic ring in the *Tbx1*$^{+/+}$ embryo (E), which is missing in the *Tbx1*$^{-/-}$ embryo (F). (G-L) Transverse histological sections of *Tbx1*$^{+/+}$ (G, I, K) and *Tbx1*$^{-/-}$ embryo (H, J, L) stained with hematoxylin and eosin at E17.5. Incus and stapes are missing in the *Tbx1*$^{-/-}$ embryo (H) as compared with the *Tbx1*$^{+/+}$ (G), see Fig. S2. s, stapes; i, incus; m, malleus. (I, J) Mandibular molar teeth are present in both the wild-type (I) and *Tbx1* mutant embryos (J). mo, molar. (K, L) Mandibular incisors are

present in both the wild-type (K) and *Tbx1* mutant embryos (L). in, incisor. Tooth abnormalities were not detected at this level of magnification.

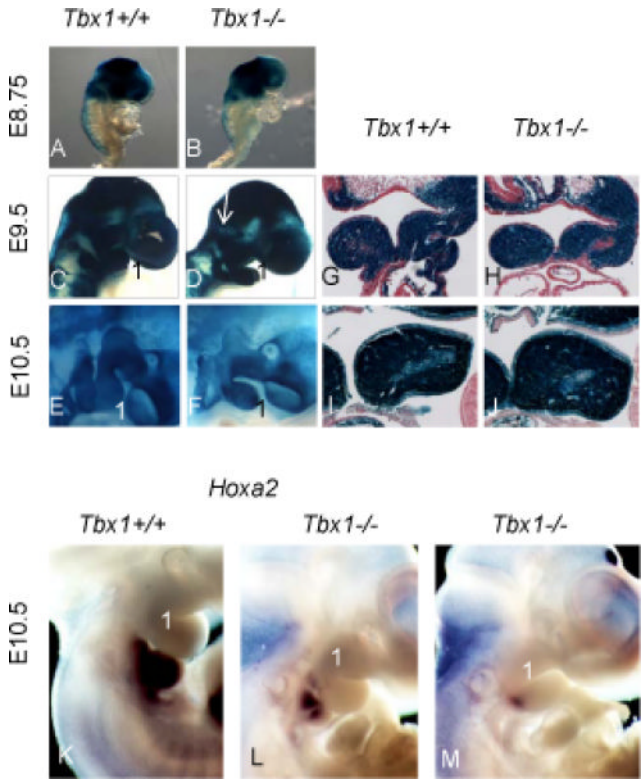

FIGURE 2. Localization of cranial neural crest cells in *Tbx1*$^{-/-}$; *Wnt1-Cre; R26R* embryos

(A-F) Lateral views of *Tbx1*$^{+/+}$*; Wnt1-Cre; R26R* (A, C, E) and *Tbx1*$^{-/-}$*; Wnt1-Cre; R26R* (B, D, F) embryos. (A, B) At E8.75, β- gal stained cells (blue) are observed in both *Tbx1*$^{+/+}$*; Wnt1-Cre; R26R* (A) and *Tbx1*$^{-/-}$*; Wnt1-Cre; R26R* (B) extending from the neural tube in two streams towards pharyngeal arch one (1) and two (2), with no observed differences between the two embryos. (C, D) At E9.5, stained cells are seen in *Tbx1*$^{+/+}$*; Wnt1-Cre; R26R* (C) and *Tbx1*$^{-/-}$*; Wnt1-Cre; R26R* (D) in the frontonasal prominence, first (1) and second (2) pharyngeal arch. Arrow marks the additional stream of NCCs that migrate into the first pharyngeal arch from rhombomere 4 as compared with wild- type embryos. Second arch is missing from null mutants. (E, F) The staining pattern in E10.5 embryos is similar to that observed at E9.5, with stained cells present throughout the pharyngeal arches. The second and third arch are missing from the null mutants.

(G-J) Histological analysis of NCCs in the pharyngeal arches of *Tbx1*$^{-/-}$*; Wnt1-Cre; R26R* embryos. *Tbx1*$^{+/+}$*; Wnt1-Cre; R26R* (G, I) and *Tbx1*$^{-/-}$*; Wnt1-Cre; R26R* (H, J) embryos were stained in whole mount for β- galactosidase activity, paraffin embedded and sectioned. Most of the cells in the first pharyngeal arch are labeled except for cells in the centre of the arch that arise from the paraxial mesoderm.

(K-M). Lateral views of whole mount in situ hybridization of embryos at E10.5 for Hoxa2 mRNA expression. Two Tbx1 -/- embryos are shown (L-M), one is more mild and has the second pharyngeal arch (L) and the other is more severe and is missing the second arch (M).

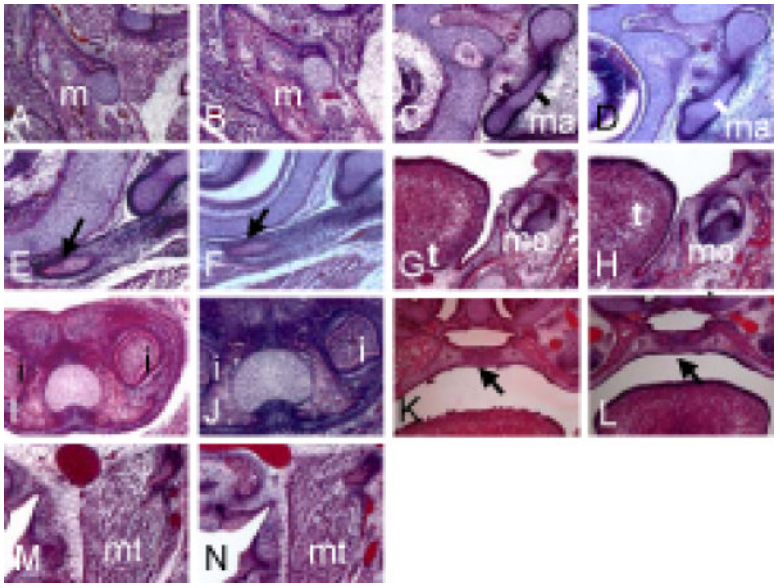

FIGURE 3. ***Wnt1-Cre; Tbx1$^{flox/-}$*** **embryos do not have a craniofacial phenotype**

(A-N) Coronal sections of *Wnt1- Cre; Tbx1$^{flox/+}$* (controls: A, C, E, G, I, K and M) and *Wnt1-Cre; Tbx1$^{flox/-}$* (NCC-KO; B, D, F, H, J, L and N) at E17.5. (A- B) There is no difference in the mandible (m) between the controls (A) and the mutant embryos (B). (C-D) Malleus (ma) is present in wildtype (C) and mutant embryos (D). (E-F) Tympanic ring (marked by arrow) forms in the controls (E) and mutant (F) embryos. (G-H) Mandibular molar teeth (mo) are present in the controls (G) and mutants (H). T, tongue. (I-J) Controls (I) as well as mutants (J) have mandibular incisors (i). (K-L) The palate is normal in the controls (K) and mutants (L). Arrow points to point of fusion of palatal shelves. (M-N) Masseter (mt), which is missing in the *Tbx1$^{-/-}$* mice, is formed in both controls (M) and mutants (N).

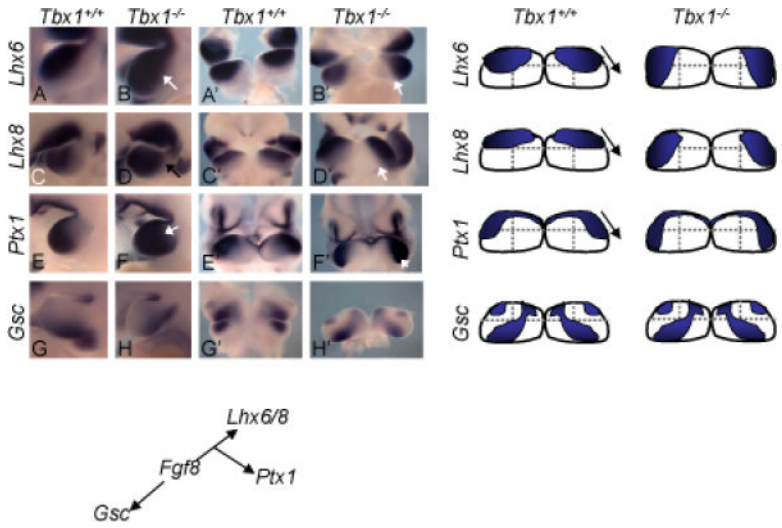

FIGURE 4. Expression of neural crest mesenchymal transcription factors in the *Tbx1*$^{-/-}$ MdPA1 at E10.5

(A- H) are lateral views of the embryos; (A'- H') are frontal views. (A, A') *In situ* hybridization showing the distribution of *Lhx6* transcripts in the mandibular arch of a *Tbx1*$^{+/+}$ embryo. (B, B') *Lhx6* is expanded into the proximal and dorsal (proximal to the arch; dorsal to the embryo) region of the mandibular arch of *Tbx1*$^{-/-}$ embryos (arrows in B, B'). (C, C') *Lhx8* expression is seen in the anterior region of the mandibular arch in *Tbx1*$^{+/+}$ embryos. (D, D') Expression of *Lhx8* is expanded in the proximo-dorsal region of the *Tbx1*$^{-/-}$ mandibular arch (arrows in D, D'). (E, E') *Ptx1* is expressed in a restricted domain of the mandibular arch of *Tbx1*$^{+/+}$ embryos. (F, F') The domain of expression of *Ptx1* is changed in the *Tbx1*$^{-/-}$ embryo, with *Ptx1* expanding in the proximo-dorsal region of the mandibular arch (arrows in F, F'). (G- H') *Gsc* is expressed in the caudal mesenchyme of the mandibular arch of the *Tbx1*$^{+/+}$ (G, G') and *Tbx1*$^{-/-}$ (H, H') embryos. Note subtle shape difference among embryos of similar genotypes (A'-H'). Right, cartoon depicting expression patterns in *Tbx1*$^{+/+}$ and *Tbx1*$^{-/-}$ embryos. Arrow shows direction of shift to proximal side of MdPA1. Below, shows previously established model of genetic pathway.

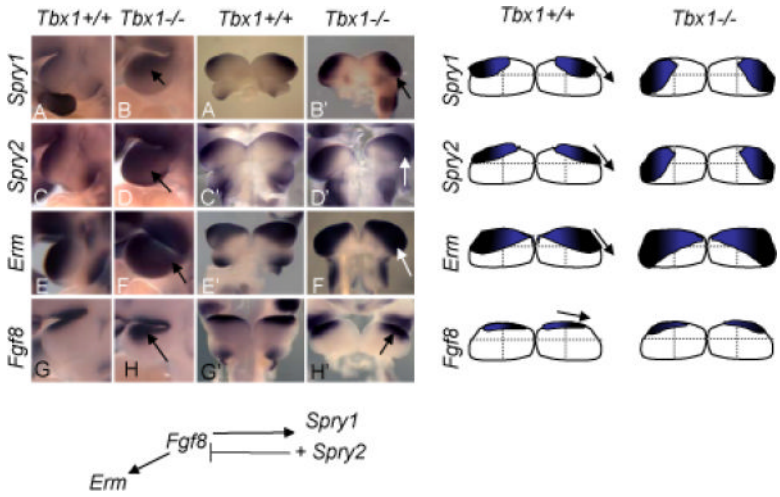

FIGURE 5. *Fgf* signaling is altered in the mandibular arches of the *Tbx1*$^{-/-}$ embryos at E10.5

(A- H) are lateral views of the embryos; (A'- H') are frontal views (A, A') *In situ* hybridization showing the distribution of *Spry1* transcripts in the mandibular arch of a *Tbx1*$^{+/+}$ embryo. (B, B') *Spry1* is expanded into the proximal and posterior region of the mandibular arch of *Tbx1*$^{-/-}$ embryos (arrows in B, B'). (C, C') *Spry2* expression is seen in the anterior region of the mandibular arch in *Tbx1*$^{+/+}$ embryos. (D, D') Expression of *Spry2* is expanded in the proximo-posterior region of the *Tbx1*$^{-/-}$ mandibular arch (arrows in D, D'). (E, E') *Erm* is expressed in a restricted domain of the mandibular arch of *Tbx1*$^{+/+}$ embryos. (F, F') The domain of expression of *Erm* is changed in the *Tbx1*$^{-/-}$ embryo, with *Erm* expanding in the posterior and proximal region of the mandibular arch (arrows in F, F'). (G, G') *Fgf8* is expressed in the proximal oral ectoderm of the *Tbx1*$^{+/+}$ embryos. (H, H') Expression of *Fgf8* is shifted in a proximo-caudal direction in the mandibular arches of the *Tbx1*$^{-/-}$ embryos (arrows in H, H'). Note varying MdPA1 shapes within genotypes. Right, cartoon depicting expression patterns in *Tbx1*$^{+/+}$ and *Tbx1*$^{-/-}$ embryos. Arrow shows direction of shift to proximal side of MdPA1. Below, shows model of previously established genetic pathway.

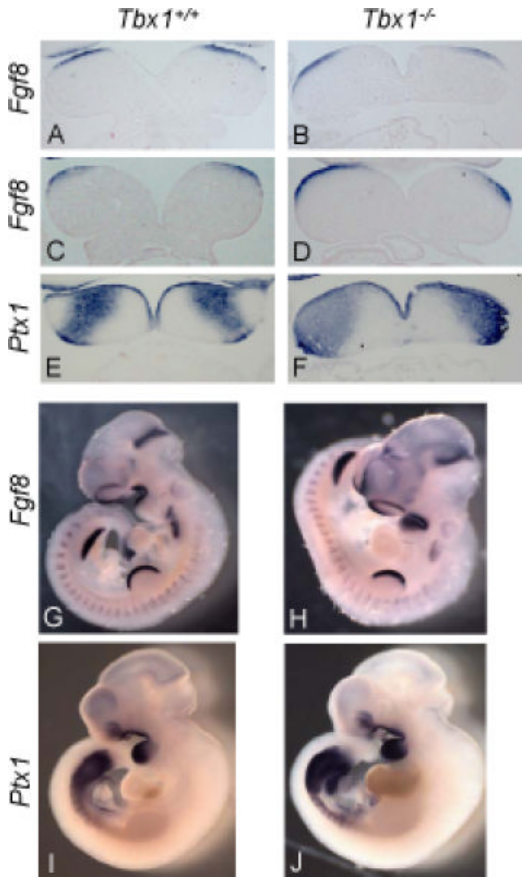

FIGURE 6. Expression of *Fgf8* is altered in the *Tbx1*$^{-/-}$ MdPA1 at E10.5

(A- F) *In situ* hybridization on coronal sections of the *Tbx1*$^{+/+}$ (A, C and E) and *Tbx1*$^{-/-}$ mutants (B, D and F) mandibular arches. (A, B) At E10.5, *Fgf8* is expressed in the proximal oral ectoderm of the mandibular arch in the *Tbx1*$^{+/+}$ embryo (A). Its expression is shifted in a proximal (lateral to the embryo) direction in the *Tbx1*$^{-/-}$ (B) embryos. (C, D) Similar expression changes are seen in the *Tbx1*$^{-/-}$ embryos (D) as compared with the *Tbx1*$^{+/+}$ embryos (C) at E9.5. (E, F) Section *in situ* hybridization also shows the expansion of *Ptx1* into the proximal region of the mandibular arch of *Tbx1*$^{-/-}$ embryo (F) compared with the wild-type (E). (G-J) Lateral views of whole mount *in situ* hybridization experiments for *Fgf8* (G, H) and *Ptx1* (I, J) in *Tbx1*$^{+/+}$ (G, I) and *Tbx1*$^{-/-}$ embryos (H, J) embryos. Additional and frontal views are in Figs. 4 and 5.

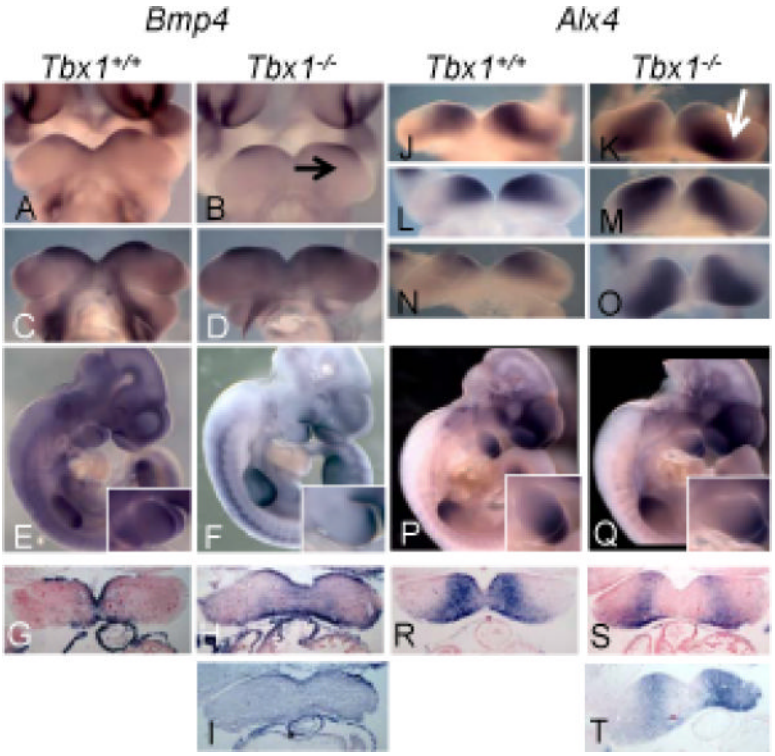

FIGURE 7. Analysis of *Bmp4* and downstream target genes in the *Tbx1*$^{-/-}$ MdPA1

(A-F, J-Q) Whole mount and (G-I; R-T) section *in situ* hybridization of *Tbx1*$^{+/+}$ (A, C, E, G, J, L, N, P, R) and *Tbx1*$^{-/-}$ (B, D, F, H, I, K, M, O, Q, S, T) embryos at E10.5. (A, C, E, G) *Bmp4* is expressed in the distal (midline) oral ectoderm of the mandibular arch of wild-type embryos. (B, D, F, H, I) Its expression is reduced but not absent in the distal midline and expanded into the proximal region of the *Tbx1*$^{-/-}$ mandibular arch. *In situ* hybridization on coronal sections shows the proximal expansion of *Bmp*4 in the *Tbx1*$^{-/-}$ mandibular arch (H, I) as compared with *Tbx1*$^{+/+}$ (G). (J, L, N, P, R) Expression of *Alx4*, a *Bmp4* target gene, is located under the *Bmp4* expression domain in *Tbx1*$^{+/+}$ embryos. (K, M, O, Q, S, T) *Alx4* is shifted proximally in *Tbx1*$^{-/-}$ embryos (arrow in K) similar to the proximal shift in *Bmp4* expression.

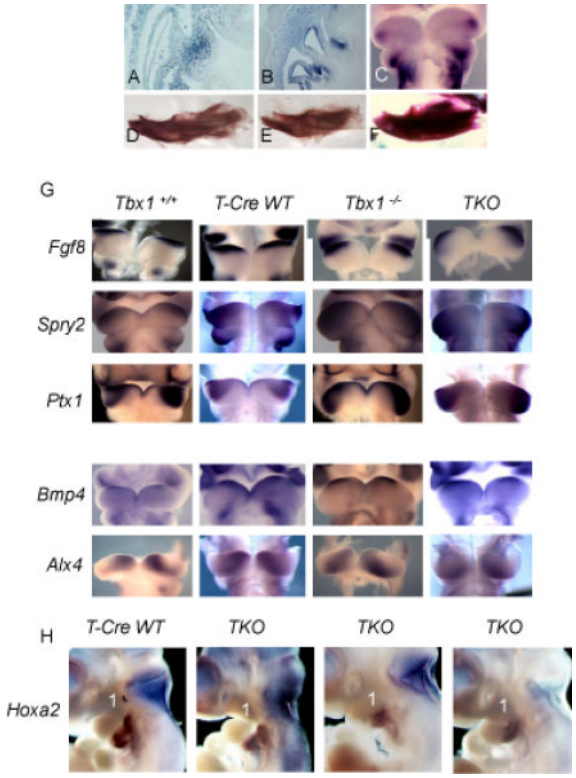

FIGURE 8. Mesodermal *Tbx1* regulates mandibular arch patterning

(A- B) *In situ* hybridization of *Tbx1* on sagittal sections at E8.5 (A), E9.5 (B) and a coronal whole mount view at E10.5 (C) show that *Tbx1* is not expressed in the oral ectoderm of the mandibular arch at the stages examined. (D-F) Skeletal preparations of E17.5 embryos showing the lateral view of a mandible of *T- Cre; Tbx1*$^{flox/+}$ (D), *T- Cre; Tbx1*$^{flox/-}$ (E) and *Tbx1*$^{-/-}$ (F) embryos. Phenotype is identical to *Tbx1*$^{-/-}$, however penetrance is reduced.

(F) Coronal views of whole mount *in situ* hybridization of E10.5, *Tbx1*$^{+/+}$, *Tbx1*$^{-/-}$, *T- Cre; Tbx1*$^{flox/+}$ (T-Cre WT) and *T- Cre; Tbx1*$^{flox/-}$ (TKO) embryos using probes for *Fgf8*, *Spry*, *Ptx1*, *Bmp4* and *Alx4*. Genes show a similar proximal shift in expression as in *Tbx1*$^{-/-}$ mutant embryos at E10.5.

(H) Whole mount views of *Hoxa2* whole mount *in situ* hybridization at E10.5. One three TKO mutants are shown with different amounts of reduction of the second pharyngeal arch, with the left being the most mild and the right being the most severe.

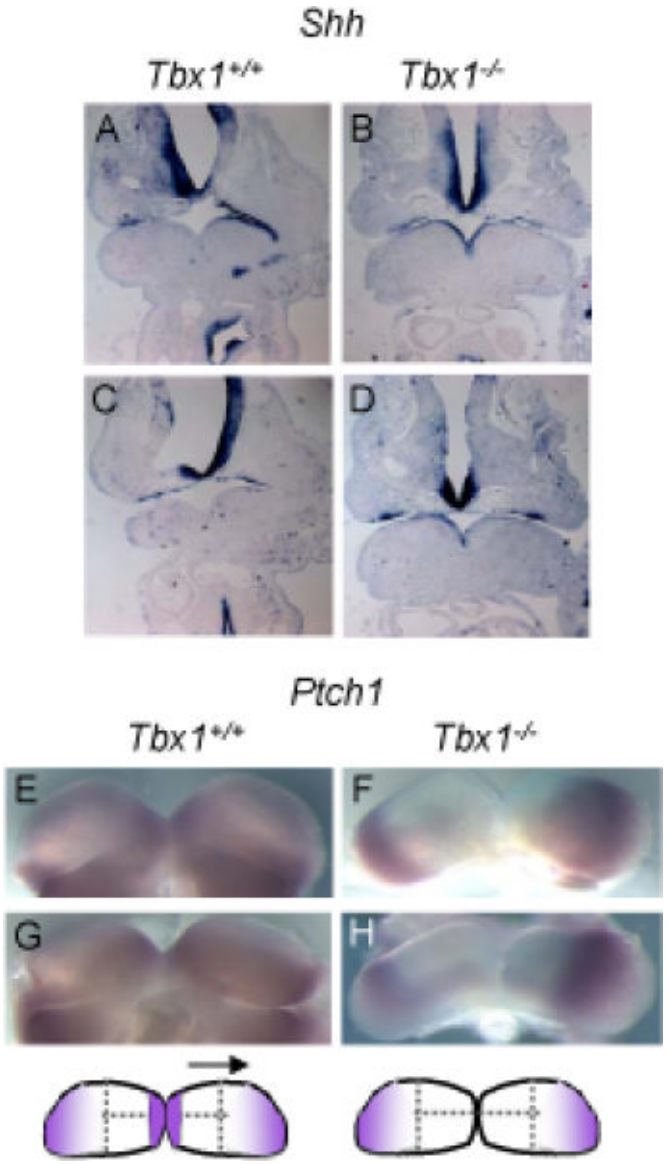

FIGURE 9. *Shh* expression is unaltered but *Ptch1* is missing from the distal midline downstream of *Tbx1* in MdPA1 at E10.5

(A- D) Coronal tissue sections from *Tbx1*$^{+/+}$ and *Tbx1*$^{-/-}$ embryos probed to detect *Shh* mRNA, shows similar expression patterns in the ventral neural tube and ectoderm of the first pharyngeal arch. (E-H) Coronal views of whole mount *in situ* hybridization of E10.5 embryos for *Ptch1*, a downstream gene of Shh. *Ptch1* expression is present in the distal midline and proximal sides of MdPA1 in *Tbx1*$^{+/+}$ embryos (E, G) but expression was reduced or missing from the distal midline in *Tbx1*$^{-/-}$ mutant embryos (F, H). Below is a cartoon illustration of the changes observed (*Ptch1* = purple).

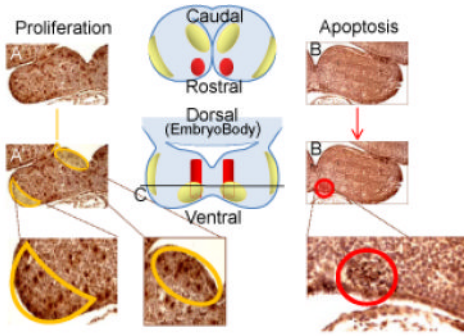

Experiment	Proliferation (cells/section)	Apoptosis (cells/section)
1	F8T37 (Control): 91.6	F8T39 (Control): 54.2
	F8T34 (KO): 148.8	F8T38 (KO): 38.7
2	F235 (Control): 259.8	F8T62 (Control): 44.6
	F236 (KO): 243.8	F8T57 (KO): 49.5
3	F8T101 (Control): 191.5	F237 (Control): 48.9
	F8T99 (KO): 159.8	F8T98 (KO): 61.9

	Proliferation (mean cell/section)	Apoptosis (mean cell/section)
Control	180.8	49.2
KO	184.1	50.0

FIGURE 10. No difference in proliferation or apoptosis between *Tbx1*$^{+/+}$ and *Tbx1*$^{-/-}$ embryos at E10.5

(A,B) Sections through location C on illustration of first arch (center). (A) At E10.5, proliferation is seen more concentrated in the yellow zones of the first arch. (B) Apoptosis is located very specifically through the medial (distal) portion of the first arch, depicted as the red zone (image). (A', B') Zones of proliferation and apoptosis are highlighted and enlarged below. (Table) Results from counting cells stained for proliferation and apoptosis are shown. Statistical analysis by T-test confirms no statistical significance in the difference between cells stained for proliferation or apoptosis in *Tbx1*$^{+/+}$ and *Tbx1*$^{-/-}$ embryos. P value was accepted at p=0.05.

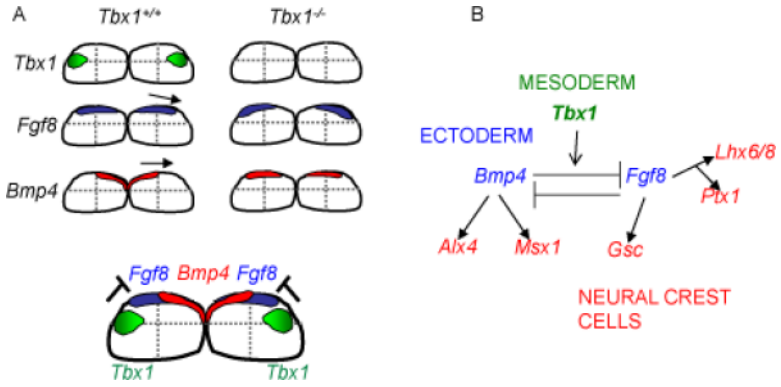

FIGURE 11. Model of *Tbx1* function in MdPA1 patterning

Cartoon shows location of Tbx1 expression in the proximal core mesoderm (green) in *Tbx1*$^{+/+}$ and *Tbx1*$^{-/-}$ embryos and E10.5. Below are expression domains of Fgf8 and Bmp4. Model shows Tbx1 restricting proximal expression domains of *Fgf8* and *Bmp4*. Genetic pathway for establishing axes forming the proximal lower jaw downstream of *Tbx1*. Genes expressed in the different germ layers comprising MdPA1 are indicated (endoderm, black; ectoderm, blue; mesoderm, green; neural crest cells, red). References for the pathway are provided in the text.